Can the Fragmentation of Hydrogen-Bonded Dimers Be Predicted: Predissociation of C_2H_2-HX[†]

Anthony J. McCaffery,*[,‡] Marisian Pritchard,[‡] and Hanna Reisler[§]

Chemistry Department, University of Sussex, Brighton BN19QJ, United Kingdom, and Department of Chemistry, University of Southern California, Los Angeles, California 90089-0482

Received: May 22, 2009; Revised Manuscript Received: November 30, 2009

HX rotational state distributions following vibrational predissociation (VP) of C_2H_2-HX (X = Cl, F, O) dimers are predicted by expressing the predissociation process as the joint probability of rovibrational excitation in the fragments following "internal collision" in the vibrationally excited dimer. Calculations of these joint probabilities for the T-shaped dimers of acetylene with HCl, DCl, HF, and OH using the angular momentum (AM) method reproduce experimental distributions with reasonable accuracy. In dimers of this complex, many different pathways for the disposal of initial energy and momentum exist in principle. The use of simple physical arguments based on (a) the direction of initial impulse upon excitation and (b) restricted relative geometries due to limited amplitude of relative motion of the dimer components allows the number of effective dissociation pathways to be much reduced. For these, the probability of rotational and rovibrational transfer into the fragments is calculated, a process that generally involves summing over a number of C_2H_2 rovibrational states for each value of j_{HX}. In calculating relative rotational populations in the fragments, it was found essential to first calculate the threshold value of available energy for that transition and the threshold value of b_n, the effective impact parameter. Without these modifications, channels of lowest j_{HX} and/or $j_{C_2H_2}$ dominate, which generally is not found experimentally. The need for these modifications is attributed to energy conservation in the dissociation and the limited range of relative orientations that the dimer pair can explore. The AM method is able to predict the very different fragment rotational excitations in this series of dimers fairly well using only readily available data. In addition, a number of new insights into the physical principles that control the dissociation of molecule−molecule dimers have emerged and are discussed. The results suggest that each fragment quantum state pair results from a very specific relative geometry of dissociation and that the balance between vibrational and rotational excitations is determined by the requirement to restrict the angular momentum "load" in the predissociation.

1. Introduction

The hydrogen bond has been described[1] as the most important of all directional intermolecular interactions, determining molecular conformation and aggregation as well as the functioning of chemical systems in different environments. Although much is known about the very diverse structures and bond strengths of H-bonded species,[1] knowledge of the microscopic mechanism of H-bond fragmentation, a process of some significance in the biological context, has proven difficult to acquire. One of the first theoretical treatments of the dynamics of H-bonding was by Coulson and Robertson in $(CH_3)_2O-HCl$,[2] though early models generally gave poor estimates of the dissociative lifetime due to neglect of fragment rotation. As experiment advanced, theoretical approaches to dimer fragmentation rapidly became more sophisticated, and Hutson et al., for example, used the close-coupled equations of scattering theory to calculate the vibrational predissociation (VP) lifetime of H_2-Ar.[3] Quantum state resolved experiments have had a major influence on the development of this field. The HF dimer, a particularly simple example of a H-bonded molecule pair, has proved to be a valuable test species through which one may trace the evolution of experimental and theoretical methods.[4,5] A recent six-dimensional, coupled channels calculation by Vissers et al.[6] predicted bound states, line widths, and rotational distributions in the HF fragments following HF stretch excitation using the potential of Klopper et al.[7] This reproduced bound state energies and obtained reasonable fits to experimental rotational state distributions. Little insight into the physics of the fragmentation process emerged, though the authors concurred with the experimental findings of Bohac and Miller[8] that excitation of dimer bend modes tends to promote fragment rotation while dimer intermolecular stretch modes favor recoil.

In a recent publication, we surveyed current theories of vibrational predissociation (VP) of van der Waals (vdW) or H-bonded molecule−atom and molecule−molecule pairs, with special emphasis on the role of angular momentum (AM), and the reader is referred to the work cited for detail.[9] For small molecules, close-coupling calculations[3,4,10] place a central role on angular momentum considerations but provide little physical insight into the factors governing its disposal. In parallel, useful propensity rules were developed by Ewing[11] and from the quantum theory of Beswick and Jortner.[12] Ewing's rules,[11] in particular, provide a guide to rotational distributions for several classes of weakly bound molecules but are by no means universal. Also, they do not deal with vibrational state specificity beyond stating that the smaller the number of quanta to be transferred the faster the rate, and angular momentum conserva-

[†] Part of the "Benoît Soep Festschrift".

* To whom correspondence should be addressed. E-mail: a.j.mccaffery@sussex.ac.uk.

[‡] University of Sussex.

[§] University of Southern California.

10.1021/jp904793d
Published on Web 12/28/2009

tion is not included. The lack of availability of multidimensional potential energy surfaces (PESs) has limited more accurate treatments for polyatomic molecules.

The focus of the current paper is on rotational excitation in the products of VP of mixed dimers of acetylene and the generation of the angular momentum required for fragment rotation. Experimental results show that (i) the process of VP in small H-bonded dimers is fairly inefficient and dissociation rates are small,[13] (ii) VP is highly state-specific, in particular in regard to fragment vibrational distributions,[5,9] and (iii) rotational distributions are usually nonstatistical, and even when they appear statistical-like, this does not indicate complete randomization of energy in the dissociating dimer.[5,9]

Unlike collision-induced state change, where the initial impact creates orbital AM, processes initiated by single-photon absorption generate only unit AM in the entrance channel. Thus, in many treatments, the high fragment j values often seen in molecular VP must be generated by interaction with the repulsive part of the PES, which possesses the required anisotropy. Here, as in previous work,[14−18] orbital AM in the entrance channel is assumed to result from an off-center internal "collision" that is converted to fragment rotation upon dissociation. This forms the basis of the internal collision AM model of McCaffery and Marsh,[17] which treats VP as a form of vibration−rotation transfer (VRT). The AM model has been shown to reproduce VRT and rotational transfer (RT) data from inelastic collisions quantitatively for many systems[14,17,19,20] and more recently was used to calculate rotational state distributions from the VP of a wide range of weakly bound atom−diatom and molecule−atom dimers.[9,17,18] It assumes that jostling among the nuclei following vibrational excitation of a dimer mode leads to an internal collision as the dimer bond contracts and the dimer components explore a range of relative geometries through intermolecular bend and stretch modes. Information on the geometry of the dimer species at the moment of dissociation can be extracted from fits to the data. Input data for the hard ellipsoid representation consist of readily available quantities such as bond length, mass, and spectroscopic constants, and a PES is not required.[14]

Detailed understanding of the fragmentation mechanism is a necessary first step in achieving predictive capability of weak bond breakage and the disposal of excess energy in the fragments, as has been shown by the pioneering work of Miller and co-workers[5,8,21,22] as well as others.[9,10,18,23−28] Recently, the experimental results for polyatomic molecules have been expanded to determine pair-correlated distributions, providing even more detailed information on the dynamics.[5,9,25−27] For example, the imaging experiments of Reisler and co-workers on several dimers (C_2H_2−HCl,[25] C_2H_2−NH_3,[26] C_2H_2−DCl,[9] and H_2O−NH_3[27]) determined rovibrational state distributions in one fragment pair-correlated with a specific rovibrational level of the other fragment. Such measurements provide rigorous tests for theories because of the removal of averaging over many quantum states,[28] and they add another dimension to the work on dimers of acetylene with HF and OH.[21−24]

Earlier analyses have revealed that several factors determine the outcome of H-bond-breaking experiments, (1) the amount of available energy the vibrationally excited species must dispose of upon fragmentation, that is, the magnitude of E_{avail}; this affects the number of states available to the fragments and the magnitude of angular momentum that has to be transferred to the fragments; (2)the array of fragment rovibrational (v;j) states accessible at each E_{avail} and the nuclear motions the different fragment vibrational species represent; (3) the initial impulse direction in the dimer species that the photon excitation induces; this determines the fragment molecule vibrational modes that may be accessed upon dissociation; and (4) the rotational quanta that may be generated upon dissociation due to the limited relative motion of the weakly bonded pair; this places limits on the extent of fragment rotational excitation in a given series of dimers.

The AM model assumes that the probability of bond breakage to a particular set of fragment vibrational and rotational states is proportional to the joint probability of rovibrational excitation in the two fragments. In general, it was shown that several acceptable exit routes exist, with each dimer geometry leading to a characteristic fragment state distribution. However, calculating the individual (and hence the joint) probabilities, even in relatively simple systems, is challenging. For the C_2H_2−HF dimer, Oudejans et al.[21] have estimated that ∼4000 potential combinations of dissociation pathways exist. Fortunately, our earlier work indicates that a number of these routes may be excluded, and in practice, relatively few combinations of fragment quantum states need be considered, though even this represents a nontrivial task.

In previous work, we were able to fit the observed fragments' rotational distributions in VP of C_2H_2−H(D)Cl and C_2H_2−NH_3 using the AM model.[9,26] Our primary objective in the present paper is to predict the relative populations of HX fragment rotational levels in the VP of a series of HX−acetylene complexes that display very different product state distributions upon VP. This series was chosen because of the extensive data sets that exist for X = F, Cl, and O and the different modes of excitation employed, that is, exciting the HX stretch or the asym-CH stretch. In these initial calculations, we only predict the global rotational distribution in the HX fragments while using experimental inputs and physical insight to reduce the number of open channels. With this approach, we obtain reasonable agreement with the experimental results. The input parameters used in the computations and the characteristic features of the VP mechanism gleaned from the simulations are discussed at the end of the paper.

The fragment rovibrational populations reported in the VP of C_2H_2−H(D)Cl[9,25−27] show that strong propensity rules exist on fragment states that may be populated, and these results will be used here to reduce the number of potential exit routes in the predictions. For example, a subset of midvalue H(D)Cl rotational states is observed for both HCl and asym-CH stretch initial excitation, and each j_{HCl} is pair-correlated with acetylene fragments in $j < 20$. Following HX vibrational excitation in C_2H_2−OH[23] and C_2H_2−HF,[21] quite different HX rotational distributions are seen. For C_2H_2−OH,[23] fragment OH rotations range from low to the maximum energetically allowed, and the distribution is bimodal. The corresponding distribution in C_2H_2−HF,[21] on the other hand, is highly distinctive with only three HF states (j_{HF} = 11, 10, 9) measurably populated. Prediction of these widely varying outcomes in VP of the acetylene dimers is the primary goal of this paper.

2. Method

The experimental evidence that preceded the formulation of the AM model of collision-induced change is described at length in a recent review.[14] Quantum state resolved experiments indicate that momentum change is the fundamental driver of inelastic processes at the molecular level, with energy change playing a constraining role set by energy conservation. In molecules, the conversion of linear to orbital and rotational angular momentum is central to most collision-induced pro-

cesses, and the probability of a collision-induced transition in its most general form is given by[14]

$$P(\Delta j, \Delta E) = P(\Delta j)P(\Delta E) \quad (1)$$

where $P(\Delta j)$ and $P(\Delta E)$ are the probability densities of AM and the energy change. In the AM model,[29] these are considered separable so that

$$P(\Delta j, \Delta E) = P(\Delta j)\delta(E_{tot} - E'_{tot})\delta(J - J') \quad (2)$$

where E_{tot} and E'_{tot} represent the total energy and J and J' the total angular momenta (rotational plus orbital) before (unprimed) and after (primed) collision. In an atom−diatomic molecule collision of reduced mass μ and relative velocity v_r, the orbital angular momentum l available for conversion to rotational AM is given by $l = \mu v b_n$, where b_n is the effective impact parameter. This expression forms the basis for a rotational transfer function that is written[29,30]

$$\int_0^{b_n^{max}} P(l|b_n)P(b_n)\delta(|E_{tot} - E'_{tot}|)\delta(|J_i - J_f|)b_n db_n dj_f \quad (3)$$

where $P(j_f|j_i)$ is the probability of transfer from the initial rotor state j_i to the final state j_f and $P(l|b_n)$ is the (conditional) probability density for generating orbital AM l given a specified b_n. The derivation of eq 3 is given in ref 30, where it is shown to predict an exponential-like fall of RT cross sections with increasing Δj. A hard ellipsoid representation, together with eq 3, gives excellent fits to a wide range of atom−diatom RT data[30] and reveals the critical parameter b_n^{max}, the maximum value of the effective impact parameter in the collision, to be of molecular dimension, being the half bond length of a homonuclear diatomic and the equivalent distances from the center of mass in a heteronuclear species. Gentry and co-workers[31] also report a similar relationship linking the rotational "rainbow" angle to the half bond length using the two-dimensional hard ellipse kinematic expressions of Bosanac.[15] The energy constraint condition on each transition will vary from process to process but is of generic form

$$\frac{1}{2}\mu v_r^2 = |\Delta E| \quad (4)$$

In practice, rather than use the probabilistic expression of eq 3, it is more convenient to generate $P(j_f|j_i)$ from a large number (>10^6) of trajectories impacting on a three-dimensional ellipsoid having the dimensions of the molecule undergoing collision, as first demonstrated by Kreutz and Flynn.[16] This hard ellipsoid representation forms the basis of all computations here. For each trajectory, the orbital angular momentum created at the ellipsoid surface is calculated and converted to molecular rotation within the constraints of state-to-state and overall energy conservation.

The similarities between VRT and VP of weakly bound dimers has led to the adaptation of the model to introduce the internal collision described above and the generation of initial orbital AM from the collision between the weakly bound fragments. Initial asym-CH stretch or HX stretch excitation of the dimer represents highly directional motion that leads to an internal collision as the dimer bond stretches and bends. The method accurately reproduces the distributions of rotational states from VP of many weakly bound atom−diatom and atom−polyatomic dimers.[17,18] In previous calculations on acetylene dimers, b_n was treated as a variable determined from best fits to experimental data.[9] The magnitude of this parameter yielded information on the geometry of the dimer at the moment of fragmentation. Analyses of the fitted fragment quantum state populations in $C_2H_2-NH_3$[11] and $C_2H_2-H(D)Cl$[9] reveal that

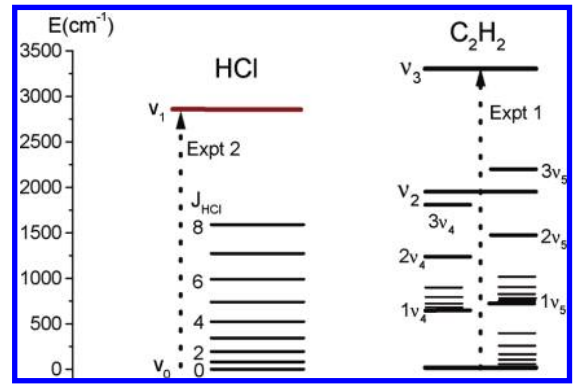

Figure 1. Energy level diagram for the dimer C_2H_2-HCl. Arrows show the two alternative forms of excitation (Expt 1 and 2) used to initiate fragmentation in this species.

dissociation occurs from the range of relative geometries in the dimer that are sampled by vibrational motions in the intermolecular modes. The lifetimes of the excited species are in the nanosecond range, and thus, the intermolecular stretch and bend vibrations explore the accessible configuration space extensively prior to dissociation.

The probability that a particular combination of fragment channels will be populated upon dissociation is the joint probability $P(v_A;j_A);P(v_B;j_B)$, where $P(v_{A(B)};j_{A(B)})$ represents the probability of populating channel $(v_{A(B)};j_{A(B)})$ in fragment A(B). Note that a third probability enters, namely, that of generating recoil orbital angular momentum $P(l_{rec})$, where l_{rec} is the magnitude of the orbital AM of recoil. This last probability is much harder to evaluate, and we discuss its role in more detail below. In the dissociation of a dimer comprising two molecules, there is no reason to suppose that a single unique exit route (i.e., a specific linked pair of fragment quantum states) would dominate. Indeed, the pair-correlated experiments show conclusively that in $C_2H_2-H(D)Cl$, numerous $(v_{C_2H_2};j_{C_2H_2})(v_{HCl};j_{HCl})$ combinations are possible. Thus, a predictive calculation of the population in a given fragment $(v;j)$ state will generally consist of the sum of the joint probabilities for a number of distinct fragmentation pathways.

Consequently, an important factor in the fragmentation process is the number and nature of fragment rovibrational energy levels available to receive energy upon dissociation, that is, those lying below E_{avail}, where E_{avail} is the available energy (=excitation energy − dissociation energy) of the dimer. For example, Figure 1 shows the energy levels of C_2H_2-HCl for the two forms of initial excitation. For clarity, not all overtones and combination bands of acetylene bend modes are displayed nor are all rotational levels shown in each species. Clearly, both bend and stretch vibrations of the C_2H_2 fragment, together with HCl and/or C_2H_2 rotation and recoil, are potential destination modes for the available energy. E_{avail} and AM must be disposed into accessible fragment rovibrational states and recoil while conserving energy and angular momentum. Fortunately, the number of open channels can be reduced in the calculations for two reasons.

First, a strong vibrational state specificity is observed in VP. In all of the T-shaped C_2H_2-HX species studied, it was observed that dissociation following asym-CH stretch excitation populates the v_2 C−C sym. stretch but not the v_4 or v_5 C_2H_2 bend modes, whereas dissociation following excitation of the HX stretch populates C_2H_2 bend modes only.[5,9,21−25] These propensities are readily justified upon considering the direction of the impulsive motion that initiates dissociation. Asym-CH stretch excitation

in the dimer comprises an initial impulse along the C_2H_2 principal axis. This form of motion is able to deliver a glancing blow to the HX species as the weak bond contracts, simultaneously interrupting the motion of the excited vibration in the process. There is no significant impulse perpendicular to the C_2H_2 molecular axis, and the result is a dephasing of the quantized oscillation and transition to the lower-energy C−C stretch together with C_2H_2 and HX rotation. When HX stretch excitation initiates dissociation, the initial impulse direction is mainly perpendicular to the C_2H_2 long axis, and both *cis*- and *trans*-C_2H_2 bend modes are excited. However, with little parallel impulse, the C−C stretch is unlikely to be accessed. Also, as shown before,[18,20] the nuclear motions involved must be such that rotational AM is generated simultaneously with vibrational state change. These observations help reduce the number of open channels. The lifetime of the excited dimer is a measure of how difficult it is to fulfill these requirements.

The second general principle that determines the importance of dissociation routes is also empirically based, though it has an element of theoretical underpinning. A common feature in the VP in the C_2H_2−HX series is that rotational excitation in the C_2H_2 fragment rarely exceeds $j_{C_2H_2} \approx 20$, even though E_{avail} allows much higher excitation. Thus, exit routes involving high rotational states of C_2H_2 likely have low probability. This limit on $j_{C_2H_2}$ suggests either that the relative geometry accessible to the dimer components is restricted such that b_n^{max}, the maximum effective impact parameter, is greatly reduced compared to that theoretically available or that the energy available for disposal as C_2H_2 rotation is limited because larger quanta, that is, C_2H_2 vibrations and HX rotations, take precedence over the smaller C_2H_2 rotations. In reality, both factors are likely to have a constraining influence.

A key parameter in the model is the maximum value of the effective impact parameter (b_n^{max}), or lever arm, about which molecular rotation is generated upon collision or via some other impulse. For situations in which collision geometry is unconstrained, this would normally be set at an appropriate molecular quantity, that is, the half bond length for a homonuclear diatomic and the equivalent distance from the center-of-mass in a heteronuclear diatomic.[14] In VP of dimers, the extent to which the full lever arm is explored depends on unknowns, such as the amplitude of intermolecular bend modes, and usually, the full theoretical b_n^{max} is unlikely to be achieved. In the present calculations, results consistent with experiment were obtained by using b_n^{thr}, the threshold value of b_n for each (v;j) channel. The b_n^{thr} values are straightforward to calculate for a given v;j channel from the threshold energy for that channel, expressed as v^{thr}, the threshold relative velocity, which is then used in the expression $b_n^{thr} = j/\mu v^{thr}$. The b_n^{thr} values vary markedly with j, rising steeply from zero at $j = 0$ to a more shallow rate of increase above $j = 4$ for the HX species. For C_2H_2, the variation of b_n^{thr} with j follows a similar form with rapid increase to $j_{C_2H_2} \approx 8$, after which it rises only very slowly. Acceptable results were obtained by setting the b_n^{thr} calculated in this manner as the maximum values in the computation for each (v;j) channel.

We also need to define the collision energy, a variable to be specified in a typical computation. Upon fragmentation, E_{avail} must be disposed into fragment rotational, vibrational, and recoil energy with zero remainder. Thus, for each rovibrational channel, we specify the collision energy for computational purposes to be that unique fraction of E_{avail} that just opens a given channel (i.e., no energy is left for recoil). This has the additional advantage of consistency in calculations carried out over a wide range of processes.

The question of recoil orbital AM and its probability density $P(l_{rec})$ was raised earlier. Little is known about the magnitude and direction of this quantity and even less regarding its probability distribution. In chemical reactions that yield low reduced mass products, energy constraints on the magnitude of l_{rec} can become the determining factor for the product rotational states that may be accessed.[32] The l_{rec} is created by the dissociating impulse at the same instant as fragment rotation, and a reasonable assumption is that its probability falls rapidly with the magnitude of l_{rec} in a manner similar to that of $P(j)$ with j. The Ewing rules,[11] which postulate that rotational excitation is generally more probable than translation, account qualitatively for the rotational distributions in the VP of several classes of vdW clusters. These rules suggest that $P(l_{rec})$ falls off somewhat faster with l_{rec} than does $P(j)$ with j, but they are not universally applicable, and the functional form of $P(l_{rec})$ is a topic that requires further investigation. Here, we calculate the probabilities for the maximum $j_{C_2H_2}$ state accessible by energy once the relevant $v_{C_2H_2}$ and j_{HCl} energies have been accounted for. This, in effect, assumes that $P(l_{rec})$ and $P(j)$ fall off at roughly equal rates with increasing magnitude of the angular momentum generated. The results of Li et al. for C_2H_2−HCl excited in the asym-CH stretch[25] show that pair-correlated high C_2H_2 rotational levels in the (v_2) C−C stretch are populated approximately uniformly, suggesting that this is a reasonable first assumption.

Calculations were performed on C_2H_2−HX dimers in which HX = HCl, DCl, HF, and OH, with dissociation initiated via the asym-CH stretch for HCl and DCl dimers and following H−X stretch excitation for HCl, HF, and OH. At this early stage in the development of a predictive approach, our focus is principally on reproducing the relative probabilities of the HX fragment rotational states.

All of the computations were performed using a modified form of the technique employed to calculate cross sections in state-to-state vibration−rotation transfer.[19] Product quantum state distributions were calculated using a Monte Carlo set of trajectories with molecules represented as hard ellipsoids having the dimensions of the species undergoing collision. In this work, C_2H_2 was simulated by an ellipsoid having semimajor and semiminor axes of length 2.12 and 0.604 Å, respectively, with a mass of 26 amu and a rotational constant $B = 1.177$ cm^{-1}. The HX species are represented as mass asymmetric ellipsoids, and input data for the calculations consist of atomic mass, spectroscopic constants, and so forth.

3. Results and Analysis

The energy level diagram of Figure 1 is drawn for the first dimer considered in this section, C_2H_2−HCl, and provides a useful guide to the other dimers discussed below since the levels of the C_2H_2 fragment are unchanged. All of the dimers in this series are T-shaped, and the dimer excitation mode strongly influences fragmentation patterns. Key quantities in the calculations are the spectroscopic parameters, that is, vibrational and rotational frequencies, the dimer excitation frequency, and the dissociation energy (D_0). These are given below for each species discussed.

(i) C_2H_2−HCl. ***(a) C−H Asym Stretch Excitation.*** The fundamental of the asym-CH stretch was excited at 3281.8 cm^{-1},[25] and since $D_0 = 700$ cm^{-1}, E_{avail} is 2582 cm^{-1}. The rotational constant of acetylene is 1.177 cm^{-1}, and that of HCl is 10.6 cm^{-1}, so that quite large amounts of energy may be absorbed into HCl rotation for relatively small AM change. As discussed above, the C−C stretch in acetylene is the preferred

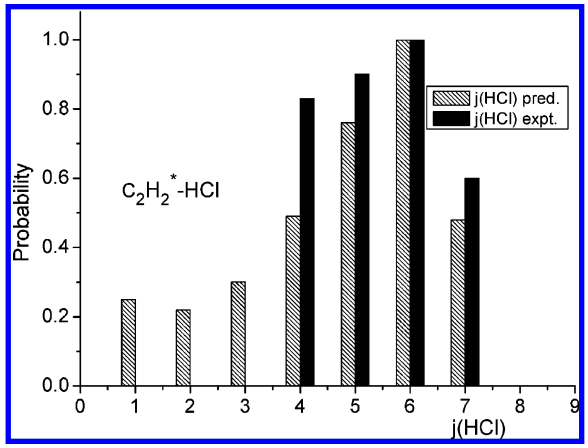

Figure 2. Experimental[25] (solid columns) and predicted (hatched columns) HCl rotational probabilities from dissociation of C_2H_2*−HCl initiated by excitation of the C−H asym stretch mode of the dimer. Note that the low j_{HCl} region is predicted to have population but experimentally is unobservable due to the presence of background HCl.

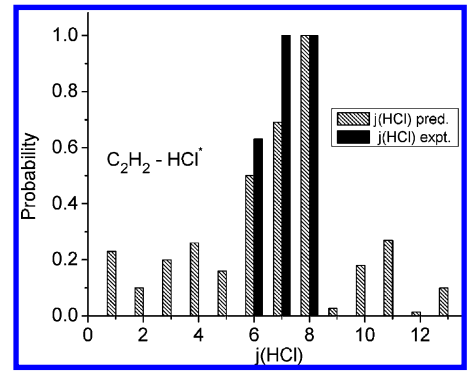

Figure 3. As that for Figure 2, but dissociation in C_2H_2−HCl is induced by HCl excitation.

mode of fragment vibrational excitation, and therefore, the bend modes υ_4 and υ_5 are ignored as potential acceptor modes. The remaining routes are (a) HCl rotation with each j_{HCl} paired with rotations of C_2H_2 in the ground vibrational state and (b) excitation of j_{HCl} paired with C_2H_2 rotations within the υ_2 C−C stretch at 1973.5 cm^{-1}. Clearly the AM "load" will be lowered in route (b) relative to that in route (a) for each j_{HCl} channel. Consider, for example, the exit route that couples $j_{HCl} = 1$ with maximum $j_{C_2H_2}$ from the energy remaining. The state $j_{HCl} = 1$ has high individual probability, but it is paired with $j_{C_2H_2} = 45$ of the vibrational ground state and hence is of very low joint probability and is ignored. This same $j_{HCl} = 1$ channel, on the other hand, is coupled with $j_{C_2H_2} = 21$ in υ_2 of C_2H_2, and although the latter channel's probability is also quite low, the high probability of $j_{HCl} = 1$ means that the joint probability for this channel is calculated to be non-negligible, as shown in Figure 2.

There is insufficient energy remaining for $j_{HCl} = 8$, 9, or 10 to pair with υ_2 C−C stretch rotational states, and energy conservation requires $j_{C_2H_2} = 38$, 36, and 34, respectively, when paired with ground-state acetylene. Thus, these j_{HCl} levels have very low relative populations. However, for $j_{HCl} = 1$−7, the coupled values of $j_{C_2H_2}$ for acetylene with C−C stretch excitation fall within the range of 4−21 and hence have nonzero joint probability. Figure 2 demonstrates that the predictions reproduce the experimental distribution obtained by Li et al.[25] reasonably well. The low j_{HCl} region is predicted to have nonzero populations, but levels below $j_{HCl} = 4$ are inaccessible to experiment due to overlap with free background HCl or from dissociation of larger clusters. The abrupt cutoff above $j_{HCl} = 7$ follows from energy conservation for exit routes involving C−C stretch fragment excitation in C_2H_2.

Calculations also demonstrate that the main experimental features of the DCl distribution from C−H asym stretch-induced dissociation of C_2H_2−DCl at $j_{DCl} = 6$, 7, 8, and 9 have the highest joint probability, as observed in the experiment,[9] though again, the probability is nonzero down to $j_{DCl} = 1$. In both cases, the C−C stretch provides the main energy dump that reduces the overall AM load. Striking similarities are found in the paired $(\upsilon;j)_{C_2H_2}$ states of these isotopomers despite the large change in vibrational and rotational quanta of the H(D)X fragment. The DCl rotational states observed experimentally are shifted upward by two j units compared to the HCl fragment, but they are similar to j_{HCl} in their respective relative populations. The reason for this is that the $(\upsilon_{C_2H_2};j_{C_2H_2})$ states paired with $j_{DCl} = 6$−9 are almost identical to those coupled to $j_{HCl} = 4$−7 upon fragmentation of C_2H_2−HCl. Note that these comments apply to the maximum accessible value of $j_{C_2H_2}$, and as described above, these are the $j_{C_2H_2}$ states for which the joint probability calculations are performed. Even though it is energetically allowed, DCl ($\upsilon = 1$) is not populated.[9]

(b) HCl Stretch Excitation. Energy of excitation in this experiment was 2806.91 cm^{-1}, and $E_{avail} = 2107$ cm^{-1},[25] around 570 cm^{-1} less than that when the C−H asym stretch was excited. The calculations become more time-consuming in this case because several acetylene bending vibrational levels may be accessed, some of which have near-degenerate components, differing in the amount of vibrational angular momentum. The data of Li et al.[25] reveal that all energetically open rotations associated with the fragment acetylene bend modes are accessed. Although the C−C stretch may initially be excluded as a potential fragment state, there are still numerous alternative exit routes, and the joint probability must be computed for each. These routes generally involve rotational states of the bend modes υ_4 and υ_5 at 612 and 730 cm^{-1}, respectively, together with their energetically allowed overtones and combination bands. In the computations for each energetically accessible j_{HCl}, all potential C_2H_2 pair states were considered and ruled out only when $j_{C_2H_2} > 20$ (except for very low j_{HX}, as discussed above). When several potential acetylene $(\upsilon;j)$ states represented possible partners for a given j_{HCl}, the joint probability of each was computed and summed to give the total contribution for that j_{HX} channel. This was commonly found to be the case since overtones and combinations of the bend modes exhibit l-type degeneracy. The results of these calculations are presented in Figure 3 together with the experimental data of Li et al.[25]

Figure 3 shows that the agreement with experiment is not as good as that for dissociation via asym-CH stretch excitation. The population ratios among the j_{HCl} levels observed by Li et al. are reasonably well reproduced by the joint probability calculations, but population is predicted in most other j_{HCl} channels albeit with lower probabilities. Low j_{HCl} are again obscured to experimental observation, but the calculations predict population in $j_{HCl} = 10$, 11, and 13, for which no intensity was observed experimentally. One possibility is that these levels, which are of small relative population, could not be observed experimentally because the upper state in the experimental detection scheme of HCl ($f^3\Delta_2$) predissociates rapidly for $j_{HCl} > 8$.[33]

(ii) C_2H_2−OH. The experimental data used to compare the C_2H_2−OH data with the calculated probabilities are those of Davey et al.,[23] who excited $\upsilon = 2$ of the OH stretch in the dimer

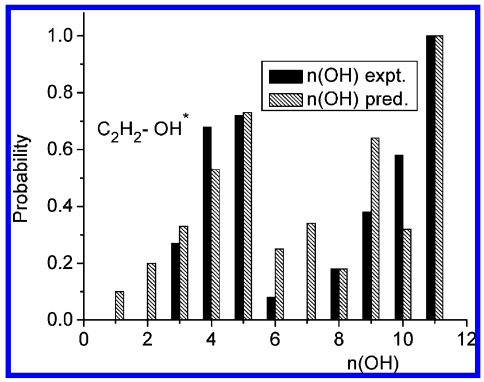

Figure 4. Experimental (solid columns) and predicted (hatched columns) rotational state probabilities of the $v = 1$ OH fragment following excitation to the OH $v = 2$ level in the C_2H_2−OH dimer. Experimental data are those of Davey et al.[23] Note that $n_{OH} = 7$ was not determined experimentally due to spectral interference.[23]

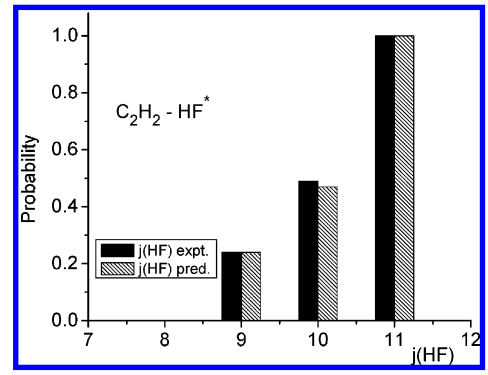

Figure 5. Experimental (solid columns) and predicted (hatched columns) rotational state probabilities of the $v = 0$ HF fragment following excitation to the HF $v = 1$ level in the C_2H_2−HF dimer. Experimental data are those of Oudejans et al.[21]

and monitored the rotational distribution in $v = 1$ of the OH fragment upon dissociation. Excitation was at 6885.5 cm^{-1}, and rotational state (n_{OH}) populations in $v = 1$ of the OH fragment were monitored by laser-induced fluorescence (LIF). The dissociation energy obtained by Davey et al. was $D_0 \leq 956$ cm^{-1}, but in our calculations, the value $D_0 = 900$ cm^{-1} was needed to predict the ratio n_{OH} =11/10 reasonably close to experiment. This value leaves 2498 cm^{-1} as the energy available to populate (v;j) levels of C_2H_2 paired with n_{OH} of $v_{OH} = 1$, the level probed by Davey et al.[23] Population of n_{OH} =11 and 10 leaves only sufficient energy to excite acetylene ground vibrational state rotations, and therefore, calculations of these relative probabilities are expected to be among the most reliable. The rotational constant of OH is 18.91 cm^{-1} (17.82 cm^{-1} for $v = 1$), almost twice that for HCl.

The method of overtone excitation has the advantage that low n_{OH} fragment populations may be determined without interference from background OH in the chamber. Population distributions in the C_2H_2 cofragments were not measured in the experiment. Experimental data are displayed in Figure 4, and the difference between this bimodal n_{OH} distribution and j_{HCl} from C_2H_2−HCl is immediately apparent. Peak populations occur at high- and mid-n_{OH}, and populations extend down to $n_{OH} = 3$. The predicted distribution, also shown in Figure 4, agrees reasonably well with the experiment. Note that the $n_{OH} = 7$ experimental data point is not measurable due to spectral interference in the LIF experiment.[23]

The n_{OH} bimodality is reproduced quite well by the calculations, and the stronger features can be clearly associated with low j states of particular C_2H_2 vibrational levels. As described above, calculations were carried out for specified n_{OH} levels and for the maximum $j_{C_2H_2}$ accessible from the energy remaining in each C_2H_2 vibrational state. Rotational states $n_{OH} = 11$ and 10 must be paired with $j_{C_2H_2}$ in the ground vibrational state, but by $n_{OH} = 9$ and 8, the AM requirements have grown well beyond $j_{C_2H_2} = 20$, and rotations in the bend fundamentals v_4 and v_5 are probably preferred. By $n_{OH} = 7$, $2v_4$ and $2v_5$ have become accessible, the latter with quite low j states, but by $n_{OH} = 6$, only relatively high j states of the bend overtones are accessible, and this is reflected in the population minimum for this state. For $n_{OH} = 5$ and 4, three quanta of the acetylene band become accessible, but the comparable intensity measurements for $n_{OH} = 4$ and 5 can only be reproduced by invoking the C−C stretch as a destination mode for $n_{OH} = 4$, in addition to the other modes. This may signify that our very useful criterion based on initial impact direction will not always be fully reliable. Low $j_{C_2H_2}$ populations drop off quite rapidly as n_{OH} continues to decrease, though they are calculated to be nonzero down to $n_{OH} = 1$.

(iii) C_2H_2−HF. Experimental data on the VP of C_2H_2−HF were obtained by Oudejans et al.,[21] and the fragmentation induced by HF stretch fundamental excitation in the dimer is considered here because it produces a very different j_{HX} distribution to those seen in the corresponding dimers of H(D)Cl and OH. The j_{HF} fragment distribution is shown in Figure 5 and is unusual in that the probability is concentrated in paired states with j_{HF} close to the energetic limit coupled with low $j_{C_2H_2}$ of ground vibrational state acetylene. The hydrogen bond in this dimer is somewhat stronger than that in other species considered here with $D_0 = 1088$ cm^{-1}. The dimer excitation frequency is 3794.4 cm^{-1}, and hence, $E_{avail} = 2706$ cm^{-1}. Rotational separations are large in HF with $B = 20.76$ cm^{-1}.

Joint probability calculations were carried out as before, with the results shown in Figure 5. Here, comparison between experiment and prediction is good, primarily because computations are quite clear-cut, with few of the routes involving fundamentals, overtones, or combinations of v_4 or v_5 able to compete with the most direct exit channel combination with $j_{HF} = 11$ and ($v_{C_2H_2}$; $j_{C_2H_2}$) = (0;3). The $j_{HF} = 10$, paired with low values of $j_{C_2H_2}$ in the vibrational ground state, also has quite high joint probability, while $j_{HF} = 9$ is able to reduce the AM load by simultaneous excitation of one of the bend modes. For lower values of j_{HF}, the joint probabilities are at least an order of magnitude smaller than that of the dominant $j_{HF} = 11$ channel. The effects of near-resonant transfer are very marked in this species, leading to population of a narrow range of fragment states at the high j_{HF} of those accessible. The larger E_{avail} in the HF case means that mid-to-low j_{HF} states are generally linked with somewhat higher $j_{C_2H_2}$ levels than those in the C_2H_2−OH dimer with resulting lowered joint probability. These two factors are primarily responsible for the striking differences in the j_{HX} distributions. The link between the simplicity of the solution to the AM and energy disposal problem and the speed of dissociation is emphasized here since the dissociative lifetime of C_2H_2−HF is nearly an order of magnitude shorter than that of other species considered here.[21]

4. Discussion and Conclusions

The goal of the present work is to provide reasonable predictions of the widely varied HX fragment rotational state distributions in the VP of C_2H_2−HX dimers by using the AM model and a consistent, justifiable set of assumptions. In previous treatments of pair-correlated data on the C_2H_2−HX

dimers, the AM method was used only to fit experimental results, and the challenge was to identify a set of parameters that would provide physical insight and yet give reasonable simulations of experimental observations. The C_2H_2-HX series was chosen because all of the dimers are T-shaped, with the polyatomic subunit providing a large number of energetically accessible final channels. Also, the results can be compared with extensive experimental data sets that include detailed pair-correlated distributions. However, predicting the relative probabilities of the dissociation pathways in these complex systems has posed several challenges, as described above.

In what follows, we first review briefly key features of the AM model and then assess the approximations and the input into the computations. The AM method focuses on the dynamics of the nuclei so that the energy of excitation of the dimer vibrational mode is in the form of nuclear motion. As a result of H-bond bend and stretch motion, an off-center internal impact occurs, generating angular momentum that, upon fragmentation, is expressed in the form of rotational and recoil orbital AM of the fragments. Quantization of fragment rovibrational levels means that conserving energy and AM throughout dissociation is complex and the excited dimers generally undergo many thousands of bend and stretch oscillations before they find the collision point, angle of impact, phase, and so forth to meet these exacting energy and AM requirements. Reducing the AM load in the fragments by populating suitable vibrational levels can simplify this problem and speed dissociation.[34]

The advantage of the procedure utilized here is that calculations are quick and, whenever tested against quantitative data, have proved to be accurate. The calculations use a 3D hard ellipsoid representation whose parameters are determined by the dimensions of the molecules under consideration, and the results of a large number of collision-induced events are computed. In addition, the method lends itself to visualization of the dissociation process using chemically familiar models so that simple rules of thumb often emerge that would be lost in more complex treatments.

Specific vibrational channels were eliminated either based on experimental results or from physical considerations based on the direction of initial impact. This served to reduce the number of open channels while still giving acceptable predictions. For each system, a spectroscopic "fingerprint" of the E_{avail} region, as, for example, in Figure 1, was an essential starting point. For polyatomic fragments, knowledge of the nuclear motions in each vibrational mode and molecular rotation (in the nonlinear case) represents valuable information in addition to level energies. In the future, it is hoped that information on fragment vibrational excitation will become available from calculations on the full PES.

In addition, it is important to recognize that in H-bonded dimers, in contrast to full inelastic collisions, bonding forces are strong enough to limit the relative geometries of the subunits and therefore severely limit b_n^{max}.[14,19] Joint probability calculations using values of b_n^{max} obtained from the bond length and position of the center-of-mass were found to predict low j_{HX} and $j_{C_2H_2}$ channels that were disproportionately dominant. Furthermore, all channels having low $j_{C_2H_2}$ were overemphasized in such calculations. We found that using b_n^{thr} improved the simulations for all of the dimers studied here, even when they generated very different fragment rotational distributions. This method also has a scaling effect that reduces the influence of overtone and combination bands of the bend modes in the probability calculations.

The principal effect of the change from an overall b_n^{max} to b_n^{thr} computed for each open channel was to change the exponentially decaying RT function into a slowly declining linear fall of $P(j)$ with j. This is not surprising since in collision-induced RT in gas-phase molecules, the origin of the exponential-like drop[35] of $P(j)$ with j lies in the exponential-like fall of $P(b_n)$ with b_n.[30] Thus, in weakly bound dimers, for which the amplitude of dimer bend modes is quite small, the above analysis indicates a unique, or at least a very limited, range of dissociation geometries for each correlated fragment pair, that is, that corresponding to the appropriate b_n^{thr} value.

Furthermore, energy must be conserved in the dissociation, and thus for each dissociation exit route, that is, the paired rotations and vibrations in the two fragments, the process must be such that E_{avail} equals exactly the amount of energy required to open the specific channels plus recoil. In calculating the joint probabilities of populating fragment rovibrational states, it was found essential to use this precise channel-opening energy as the (internal) collision energy to achieve best agreement with the experimental results.

These initial attempts at predicting the rotational distributions in these hydrogen-bonded dimers can be considered reasonably successful. The principal features of the widely varying distributions are reproduced though, with the exception of C_2H_2-HF, the channel relative populations are rarely predicted with precision. However, since the calculations generally involve summation over contributions from each j_{HX} state together with a significant number of paired C_2H_2 rovibrational states, exact agreement with experiment was not expected. Also, no exit channel effects that depend on a specific PES can be included in a treatment that makes no reference to a potential and is based on the mechanics of momentum interconversion. The influence of PES exit channel effects should be much less pronounced here than that in photodissociation from repulsive states of covalently bound molecules.[36] The predictions are expected to be best when the range of coupled states available to the fragments is small, that is, when E_{avail} is small or the density of potential fragment state is sparse, or when a small number of paired exit channels dominate, as found in C_2H_2-HF.

In conclusion, we find that the AM model predicts the very different fragment rotational excitations in this series of dimers quite well. In addition, a number of interesting new insights into the physical principles that control the dissociation of molecule−molecule dimers have emerged. The constrained dimer geometry appears to be a significant factor in determining fragment rotational state distributions, as is the need of the dimer to meet the requirements of energy and AM conservation. The calculations suggest that dissociation occurs when threshold conditions of energy and b_n, the effective impact parameter, are achieved. This indicates that specific relative geometries of the dimer components lead to narrow quantum state distributions in the fragments. In agreement with previous results, we find that excited species prefer to dissociate via fairly low fragment angular momentum routes, a process not always compatible with the disposal of large amounts of energy. Depositing energy into fragment vibrations can lower the overall AM load, and this appears to be a common strategy adopted by excited dimers. In the series of acetylene−HX dimers examined here, the energy and angular momentum disposal algorithm is simplest in the C_2H_2-HF species following HF stretch excitation, and it is not surprising that this dimer dissociates approximately an order of magnitude faster than the others considered here.

Although the number of H-bonded dimers considered here is small, the significant differences in dissociative lifetime and

state distributions following HX activation deserve further comment. In each case, there are exit routes that pair the rotationally excited, ground vibration state of C_2H_2 with high HX rotations. While this provides the overwhelmingly dominant channel for C_2H_2-HF fragmentation, it is only one of several strong channels in C_2H_2-OH and is not seen experimentally in C_2H_2-HCl (though it is predicted to be nonzero in our calculations, and its absence in the experiment might be a result of spectroscopic difficulties). It appears from our analysis that routes that keep the AM load low are preferred, and beyond a certain *j* value for a specific system, vibrational energy transfer becomes more probable. However, the difference between success and failure appears to be quite small.

Acknowledgment. H.R. thanks Dr. Andrew Mollner for critical reading of the manuscript and gratefully acknowledges support by the U.S. National Science Foundation.

References and Notes

(1) Steiner, T. *Angew. Chem., Int. Ed.* **2002**, *41*, 48.
(2) (a) Coulson, C. A.; Robertson, G. N. *Proc. R. Soc. London, Ser. A* **1974**, *337*, 167. (b) Coulson, C. A.; Robertson, G. N. *Proc. R. Soc. London, Ser. A* **1975**, *342*, 289.
(3) (a) Hutson, J. M.; Ashton, C. J.; LeRoy, R. J. *J. Phys. Chem. A* **1983**, *87*, 2713. (b) Hutson, J. M. *Annu. Rev. Phys. Chem.* **1990**, *41*, 123.
(4) (a) Halberstadt, N.; Brechignac, P.; Beswick, J. A.; Shapiro, M. *J. Chem. Phys.* **1986**, *84*, 170. (b) von Dirke, M.; Bacic, Z.; Zhang, D. H.; Zhang, J. Z. H. *J. Chem. Phys.* **1995**, *102*, 4382. (c) DeLeon, D. I.; Muenter, J. S. *J. Chem. Phys.* **1984**, *80*, 6092.
(5) Oudejans, L.; Miller, R. E. *Annu. Rev. Phys. Chem.* **2001**, *52*, 607, and references therein.
(6) Vissers, G. W. M.; Groenenboom, G. C.; van der Avoird, A. *J. Chem. Phys.* **2003**, *119*, 227–286.
(7) Klopper, W.; Quack, M.; Suhm, M. A. *J. Chem. Phys.* **1988**, *108*, 10096.
(8) Bohac, E. J.; Miller, R. E. *J. Chem. Phys.* **1993**, *99*, 1573.
(9) Pritchard, M.; Parr, J.; Li, G.; Reisler, H.; McCaffery, A. J. *Phys. Chem. Chem. Phys.* **2007**, *9*, 6241–6252.
(10) Rohrbacher, A.; Halberstadt, N.; Janda, K. C. *Annu. Rev. Phys. Chem.* **2000**, *51*, 405.
(11) (a) Ewing, G. *J. Chem. Phys.* **1979**, *71*, 3143;(b) Ewing, G. *J. Chem. Phys.* **1980**, *72*, 2096.
(12) Beswick, J. A.; Jortner, J. *Adv. Chem. Phys.* **1981**, *47*, 363.
(13) Miller, R. E. *Acc. Chem. Res.* **1989**, *23*, 10.
(14) McCaffery, A. J. *Phys. Chem. Chem. Phys.* **2004**, *6*, 1637, and references therein.
(15) Bosanac, S. *Phys. Rev. A* **1981**, *26*, 816.
(16) Kreutz, T. G.; Flynn, G. W. *J. Chem. Phys.* **1991**, *93*, 452.
(17) McCaffery, A. J.; Marsh, R. J. *J. Chem. Phys.* **2002**, *117*, 9275.
(18) Sampson, R. K.; Bellm, S. M.; McCaffery, A. J.; Lawrance, W. D. *J. Chem. Phys.* **2005**, *122*, 074311.
(19) Marsh, R. J.; McCaffery, A. J. *J. Phys. B* **2003**, *36*, 1363.
(20) McCaffery, A. J.; Osborne, M. A.; Marsh, R. J.; Lawrance, W. D.; Wacklawik, E. J. *J. Chem. Phys.* **2004**, *121*, 169.
(21) (a) Oudejans, L.; Moore, D. T.; Miller, R. E. *J. Chem. Phys.* **1999**, *110*, 209. (b) Oudejans, L.; Moore, D. T.; Miller, R. E. *J. Chem. Phys.* **1999**, *110*, 7109.
(22) (a) Huang, Z. S.; Miller, R. E. *J. Chem. Phys.* **1987**, *86*, 6059. (b) Huang, Z. S.; Miller, R. E. *J. Chem. Phys.* **1989**, *90*, 1478.
(23) Davey, J. B.; Greenslade, M. E.; Marshall, M. D.; Lester, M. I.; Wheeler, M. D. *J. Chem. Phys.* **2004**, *121*, 3009.
(24) (a) Marshall, M. D.; Lester, M. I.; Wheeler, M. D. *J. Chem. Phys.* **2004**, *121*, 3019. (b) Marshall, M. D.; Davey, J. B.; Greenslade, M. E.; Lester, M. I. *J. Chem. Phys.* **2004**, *121*, 5845.
(25) Li, G.; Parr, J.; Fedorov, I.; Reisler, H. *Phys. Chem. Chem. Phys.* **2006**, *8*, 2915.
(26) Parr, J.; Li, G.; Federov, I.; McCaffery, A. J.; Reisler, H. *J. Phys. Chem. A* **2007**, *111*, 7589.
(27) (a) Mollner, A. K.; Casterline, B. E.; Ch'ng, L. C.; Reisler, H. *J. Phys. Chem. A* **2009**, *113*, 10174. (b) Mollner, A. K.; Casterline, B. E.; Ch'ng, L. C.; Reisler, H. *J. Phys. Chem. A* **2009**, doi: 10.1021/jp91008f.
(28) Reisler, H. *Annu. Rev. Phys. Chem.* **2009**, *60*, 39.
(29) McCaffery, A. J.; Al Wahabi, Z. T.; Osborne, M. A.; Williams, C. J. *J. Chem. Phys.* **1993**, *98*, 4586.
(30) Osborne, M. A.; McCaffery, A. J. *J. Chem. Phys.* **1994**, *101*, 5604.
(31) Hoffbauer, M. A.; Burdenski, S.; Giese, C. F.; Gentry, W. R. *J. Chem. Phys.* **1983**, *78*, 3832.
(32) McCaffery, A. J. *J. Chem. Phys.* **2008**, *129*, 224303.
(33) Callaghan, R.; Arepalli, S.; Gordon, R. J. *J. Chem. Phys.* **1987**, *78*, 3832.
(34) McCaffery, A. J.; Marsh, R. J.; Osborne, M. A. *J. Phys. Chem.* **2005**, *109*, 5005.
(35) Brunner, T. A.; Pritchard, D. *Adv. Chem. Phys.* **1982**, *50*, 589.
(36) Schinke, R. *Photodissociation Dynamics*; Cambridge University Press: Cambridge, U.K., 1993.

JP904793D